A 3D Printed Microfluidic Device for Scalable Multiplexed CRISPR-Cas12a Biosensing

Kathrine Curtin[1], Jing Wang[2], Bethany J. Fike[2], Brandi Binkley[2], Peng Li[2*]

[1] Department of Mechanical and Aerospace Engineering, West Virginia University, Morgantown, WV, USA

[2] C. Eugene Bennett Department of Chemistry, West Virginia University, Morgantown, WV, USA.

* Correspondence and requests for materials should be addressed to P.L. (peng.li@mail.wvu.edu)

Abstract

Accurate, rapid, and multiplexed nucleic acid detection is critical for environmental and biomedical monitoring. In recent years, CRISPR-Cas12a has shown great potential in improving the performance of DNA biosensing. However, the nonspecific *trans*-cleavage activity of Cas12a complicates the multiplexing capability of Cas12a biosensing. We report a 3D-printed composable microfluidic plate (cPlate) device that utilizes miniaturized wells and microfluidic loading for a multiplexed CRISPR-Cas12a assay. The device easily combines loop-mediated isothermal amplification (LAMP) and CRISPR-Cas12a readout in a simple and high-throughput workflow with low reagent consumption. To ensure the maximum performance of the device, the concentration of Cas12a and detection probe was optimized, which yielded a four-fold sensitivity improvement. Our device demonstrates sensitive detection to the fg/mL level for four waterborne pathogens including shigella, campylobacter, cholera, and legionella within 1 hour, making it suitable for low-resource settings.

Keywords: microfluidic, CRISPR, biosensor, Cas12a, molecular diagnosis**,** waterborne pathogen

Introduction

Nucleic acids, such as RNA, DNA, and miRNAs, are valuable biomarkers for disease diagnosis and monitoring. Next-generation sequencing (NGS), microarray, and polymerase chain reaction (PCR) are widely used technologies for nucleic acid screening; however, they suffer from long turnaround times and are costly.[1,2] Clustered regularly interspaced short palindromic repeats (CRISPR) associated effectors such as Cas12a and Cas13a-d are promising alternative technologies for nucleic acid biosensing because of their fast reaction times, specificity, and sensitivity to DNA or RNA.[3,4] In CRISPR-Cas biosensing, Cas nucleases recognize nucleic acid targets by complementary binding with CRISPR guide RNA (crRNA). Upon binding, the nuclease is activated and triggers collateral cleavage activity, cleaving non-targeting DNA. This mechanism is used for biosensing by adding single-stranded fluorophore-quencher DNA reporters to generate a detectable fluorescence signal when cleaved by the Cas collateral activity.[5,6] CRISPR-Cas is typically coupled with preamplification to improve detection sensitivity, such as recombinase polymerase amplification (RPA)[7–9] and loop-mediated isothermal amplification (LAMP)[10–12]. CRISPR-Cas biosensing offers high sensitivity and specificity because of the highly specific crRNA-DNA or RNA target binding event, which can discriminate single nucleotide variations.[13] CRISPR-Cas assays have become a powerful diagnostic tool for pathogens and viruses because they have achieved 10^{-18} M sensitivities[14–17] with detection times as fast as less than one hour.[8,10,18,19] Coupled with simple workflow and operation steps, these advantages make CRISPR-Cas assays suitable for rapid point-of-care (POC) diagnostics.

Multiplexed nucleic acid assays are paramount in clinical settings since they improve diagnostic power, save time, and reduce costs. Many infectious diseases present with similar symptoms. Therefore, screening a panel of pathogen markers is essential in identifying bacterial or viral sources, such as in respiratory infections or water and foodborne illnesses. However, multiplexing CRISPR-Cas reactions is difficult. Because of the non-specific *trans*-cleavage activity of Cas effectors, multiplexing can only be achieved by physically separating CRISPR-Cas reactions with respective targets.[20,21] This requirement results in using many individual reaction tubes or wells and extensive manual steps to screen a single sample for multiple targets. Few examples of multiplexed CRISPR-Cas assays have been presented. SHERLOCKv2 was developed using four CRISPR enzymes (LwaCas13a, PsmCas13b, CcaCas13b, and AsCas12a), each specific with *trans*-cleavage for four fluorescent probes.[19] CARMEN was developed by using droplet technology to space-encode and color-code multiplexed reactions to expand the number of targets.[22] A microfluidic device, MiCar, has also demonstrated multiplexing by compartmentalizing CRISPR reactions into reaction chambers so multiple targets could be measured on a single device.[7] While these systems can measure many targets, they are unsuitable for the point-of-care (POC) because they require off-device sample preparation, droplet generation, and complex operation. Recently, Hu et al. presented a CRISPR-based reverse dot blot assay that uses sandwich DNA probes to detect four targets in parallel on a microfluidic device.[23] However, the horizontal microfluidic design requires many microfluidic channels to analyze samples, limiting the number of total reactions on the device. Currently, there are no CRISPR-Cas assays available that can detect many targets with low cost and simple operation at the POC.

To achieve scalable multiplexing CRISPR-Cas biosensing without the need of external equipment, we present a 3D-printed composable microfluidic plate (cPlate) device composed of miniatured microwells and a microchannel loading system. We previously demonstrated the feasibility of using cPlate-based fluid manipulation to achieve multiplexed ELISA.[24] In this work, we modified our cPlate design to achieve all the necessary fluid operation of multiplexed LAMP amplification and CRISPR-Cas12a biosensing without any external fluid manipulation units. The present cPlate device is a miniaturized 96-microwell plate that overcomes CRISPR-Cas12a multiplexing challenges by separating amplification and detection for each target into single reaction wells. The device design and operation are user-friendly and enable up to 96 individual reactions to be performed on a single device simultaneously. Horizontal and vertical microfluidic loading systems easily load amplification and CRISPR reagents into the device with high precision and without excessive manual steps. Additionally, the cPlate does not require external power sources or technical equipment for loading or operation. Rather, it is easily loaded by micro pipetting, and sequential reactions are initiated by assembling the plates by hand. The utility of the present device was demonstrated by screening a panel of common waterborne pathogens in one device. The device's simple operation and high performance offer an important step toward translating CRISPR-Cas12a-mediated reactions to the POC.

Experimental

Materials and Reagents

Poly (ethylene glycol) diacrylate (PEGDA, MW 250), phenylbis (2,4,6-trimethylbenzoyl) phosphine oxide (Irgacure 819),). 2-nitrophenyl phenyl sulfide (NPS) was purchased from TCI (Tokyo, Japan). Ultra-Ever Dry super-hydrophobic coating was purchased from Ultratech (San Jose, CA, USA). Epoxy glue (5-minute epoxy, Devcon) was purchased from ITW (Glenview, IL, USA). Food color was purchased from Wilton Industries. Water was purified using a Merck Millipore purification system (Bedford, MA, USA). WarmStart® LAMP Kit, NEBuffer™ r2.1, and nuclease-free water were purchased from New England Biolabs ® (Ipswich, MA, USA). All primers, DNA and RNA sequences, and Alt-R™ L.b. Cas12a (Cpf1) Ultra were purchased from Integrated DNA Technologies (Coralville, IA, USA). crRNA sequences were selected using Benchling and cross-referenced using NCBI BLAST.

Device fabrication

The microfluidic devices were fabricated by an Asiga Pico2 HD 3D printer with an LED peak wavelength of 385 nm, an X-Y plane resolution (pixel size) of 37 μm, and a Z-axis control of 1 μm. The 3D microfluidic device structures were designed by SolidWorks and uploaded to the 3D printer. The detailed design of channel plates and well plates are shown in Figure S1. The printing material for well plates was PEGDA 250 with 0.5% (w/w) Irgacure 819, which is photocurable and generates colorless structures. For channel plates, PEGDA 250 with 0.5% (w/w) Irgacure 819 and 0.5% (w/w) NPS was used. NPS served as an absorber to control the penetration depth of the incident light and enabled printing of the microchannels inside the chip. We set the build layer thickness as 50 μm, with the exposure time of each layer as 0.3 s for well pates and 1 s for channel plates.

After the 3D printing was completed, the plates were immediately removed from the build plate and flushed with IPA to dissolve the unpolymerized material. The plates were then cured by exposing them to UV light (365 nm) for 5 min. To enhance the transparency of the device and enable microscope observation, the printed plates were fastened onto glass slides with epoxy glue.

To confine the liquid in the microfluidic channels and avoid leakage and cross-contamination during the plate assembly process, a superhydrophobic coating was applied to the outer surfaces of the channel plates and well plates. Ultra-Ever Dry superhydrophobic coating reagent was applied in two coating steps. The bottom coat bonded to the material surface, and the topcoat created a hydrophobic surface repelling the water. An airbrush sprayer was used to apply the two coating reagents and produce uniform layers on the device surfaces. To avoid unwanted coating on the surfaces of the wells, shield structures were 3D printed and assembled into the wells of the plates. The bottom coating was dried for 30 min, and the top coating was dried for 2 h. After coating, all devices were washed with water and dried with gentle airflow.

Device Temperature Stability Analysis
Two plates were both loaded with an aqueous fluorescein solution and assembled. The fluorescence intensity was measured across the wells using a Zeiss inverted fluorescence microscope. The device was then heated to 65°C for 30 minutes, and the fluorescence intensity of the wells was measured.

Standard LAMP Assay and Validation of LAMP Amplification
The standard LAMP amplification was conducted using the WarmStart® LAMP Kit from NEB. In brief, a 25 µL solution containing 12.5 µL of WarmStart® LAMP mix, 0.5 uL SybrGreen, 2.5 µL primer mix, 2 µL target, and 7.5 µL nuclease-free water was prepared for each target. A solution containing no target and 2 µL of nuclease-free water served as a non-template control. The reaction was incubated for 30 minutes at 65°C using a Benchmark Thermal Cycler. After incubation, fluorescence was measured using a Zeiss inverted fluorescence microscope. Additionally, the products were analyzed using 1% agarose gel electrophoresis. Gel electrophoresis was done using a MyGel Mini Electrophoresis System from Accuris Instruments, and the DNA samples were separated under 50 V for 1 hr.

Validation of the Loading and Fluid Manipulation
The standard LAMP reaction mix was prepared for cholera and loaded vertically into the cPlate. 1 ng/mL of cholera sample and DI water were loaded into the alternating rows of a second plate. The two plates were assembled, secured with adhesive tape, and then heated to 65°C for 30 minutes. The fluorescence intensity of the rows was measured using a Zeiss inverted fluorescence microscope with a Andor Zyla 4.2 sCMOS camera. The mean and coefficient of variation for each row were calculated.

500 nM RNP complexes were prepared for cholera by combining 1 µM L.b. Cas12a with 1.25 µM of respective crRNA. The RNP complex was combined with 2 µM reporter probe and loaded vertically into the cPlate. Alternating rows containing cholera LAMP

amplicons and DI water were loaded horizontally into the sample plate. The LAMP and CRISPR plates were assembled and secured with adhesive tape, and fluorescence intensity was measured using a Zeiss inverted fluorescence microscope every 5 minutes for 30 minutes. The mean and coefficient of variation for each row after 30 minutes were calculated.

To assess well volume consistency, plate rows were loaded with alternating Alexa-488 dye solution and DI water using the row-loading plate. After loading, the plate was assembled with a plate containing 0.25 mm shallow wells to remove excess liquid. Then, a fluorescence image of the plate was taken using a ChemiDoc MP imager, Bio-Rad. The fluorescence intensity across the rows was analyzed using the matched software.

Cross-reactivity evaluation for gRNA

500 nM RNP complexes were prepared for the 4 targets by combining 1 μM L.b Cas12a with 1.25 μM of respective crRNA. LAMP amplicons for each target were loaded horizontally into the sample plate. The RNPs and 2 μM reporter probe were loaded vertically into the CRISPR plate. The reaction was incubated at room temperature for 30 minutes with fluorescence measurements at 5-minute intervals.

Ribonucleoprotein (RNP) Concentration Optimization

The Cas12:crRNA concentration, or RNP concentration, was optimized by fluorescent monitoring for each crRNA and waterborne pathogen target. RNPs were prepared by combining 1 μM L.b Cas12a with 1.25 μM of respective crRNA to bring the final concentration of RNPs to 275 nM, 630 nM, or 1 μM in NEBuffer™ r2.1. The solution was incubated at 37°C for 2 hours.

An 18 μL CRISPR-Cas12a reaction mixture was prepared by mixing 275 nM, 630 nM, or 1 μM L.b. Cas12a, 275 nM, 630 nM or 1 μM crRNA, 2 μM reporter probe, and 1× NEBuffer™ r2.1. The reaction was then initiated by the addition of 1 ng/mL of cholera LAMP amplicon to bring the total reaction volume to 20 μL. A reaction without target addition was used as the non-template control. Reactions with varied concentrations of RNP were conducted at room temperature and monitored by fluorescent measurement every 5 minutes using a Zeiss inverted microscope. The reactions were observed for a total of 30 minutes.

Fluorescent Reporter Probe Concentration Optimization

RNPs were prepared by combining 1 μM L.b Cas12a with 1.25 μM of respective crRNA to bring the final concentration of RNPs to 630 nM in NEBuffer™ r2. The solution was incubated at 37°C for 2 hours.

Reporter probe optimization was conducted by fluorescence monitoring in the cPlate.18 μL CRIPSR reaction mixtures containing 630 nM RNP, 1 μM, 1.25 μM, 1.5 μM, 2 μM, 4.75 μM, or 6 μM reporter probe, and 1× NEBuffer™ r2.1 were prepared. The reaction was then initiated by the addition of 1 ng/mL of LAMP cholera amplicon bringing with total reaction volume to 20 μL. A reaction without target addition was used as the non-template control. Reactions with varied concentrations of reporter probe (1 μM, 1.25 μM, 1.5 μM,

2 μM, 4.75 μM, and 6 μM) were conducted at room temperature and monitored by fluorescent measurement every 5 minutes using a Zeiss inverted microscope. The reactions were observed for a total of 30 minutes.

Device Operation Principle for Single and Multiplexed Targets

The principle and operation of the multiplexed cPlate microfluidic are visualized in Figure 1. Briefly, the samples containing target DNA are loaded into the rows of the sample plate using the horizontally loading channel plate. A row is loaded with nuclease-free water to serve as a non-template control. A modified WarmStart® LAMP reaction mix was prepared for each target reaction. 10 μL of 10x primer mix was combined with 25 μL of WarmStart® master mix. Then, the LAMP amplification mix containing the target primers and WarmStart® master mix is loaded onto the LAMP plate using the vertically loading channel plate. The sample plate and LAMP plate are carefully assembled using the corner holes and posts as a guide. The plates are gently secured using adhesive tape and placed in a thermal cycler for 30 minutes to 65°C.

After isothermal amplification, the sample and LAMP plates are dissembled, and the LAMP plate is stored in a humified environment until assembly with the CRISPR plate. CRISPR-Cas12a reaction mixes were prepared by preparing a solution 4.75 μM fluorescence probe and 630 nM RNP. The reaction mix for each target was then loaded into the respective columns on the CRISPR plate using the vertically loading channel plates. Using the corner holes and posts on the plates as a guide, the LAMP plate and CRISPR are gently assembled, allowing the fluid from each well to merge with its complimentary well. The two plates were secured together using adhesive tape. Fluorescent measurements were acquired every 5 minutes for 30 minutes. Device loading patterns are visualized in Figure S2.

Results and Discussion

Working principle

A well plate is a convenient platform to physically separate CRISPR-Cas12a reactions for multiplexing. However, many manual operations or robotics are necessary to process each reaction. Therefore, the number of manual operations increases linearly with an increasing number of reactions. The number of operations will further increase with the increase of sample processing steps, which hinders its application in POC settings. Here, we utilized the cPlate strategy to achieve simultaneous fluid manipulation in each individual microwell without the need of external equipment.

The cPlate assay uses three identical well plates and two channel loading plates (Figure 1a). All plates were surface modified with a superhydrophobic coating to facilitate fluid loading and prevent well cross-contamination. One well plate is designated for each step in the workflow: sample, LAMP reaction, and CRISPR-Cas reaction. Sample and subsequent LAMP and CRISPR reagent loading into each well was achieved by assembling channel plates with well plates by hand. Once assembled and secured, the fluid is dispensed via a micropipette into the channel inlet. The fluid flows through the channel plate and fills the wells, so when the plates are disassembled, the fluid remains in the well plate. The channel plates are patterned with two different loading

configurations. The horizontal loading configuration enables the rows of the well plate to be individually loaded, while the vertical loading configuration enables column loading (Figure 1b).

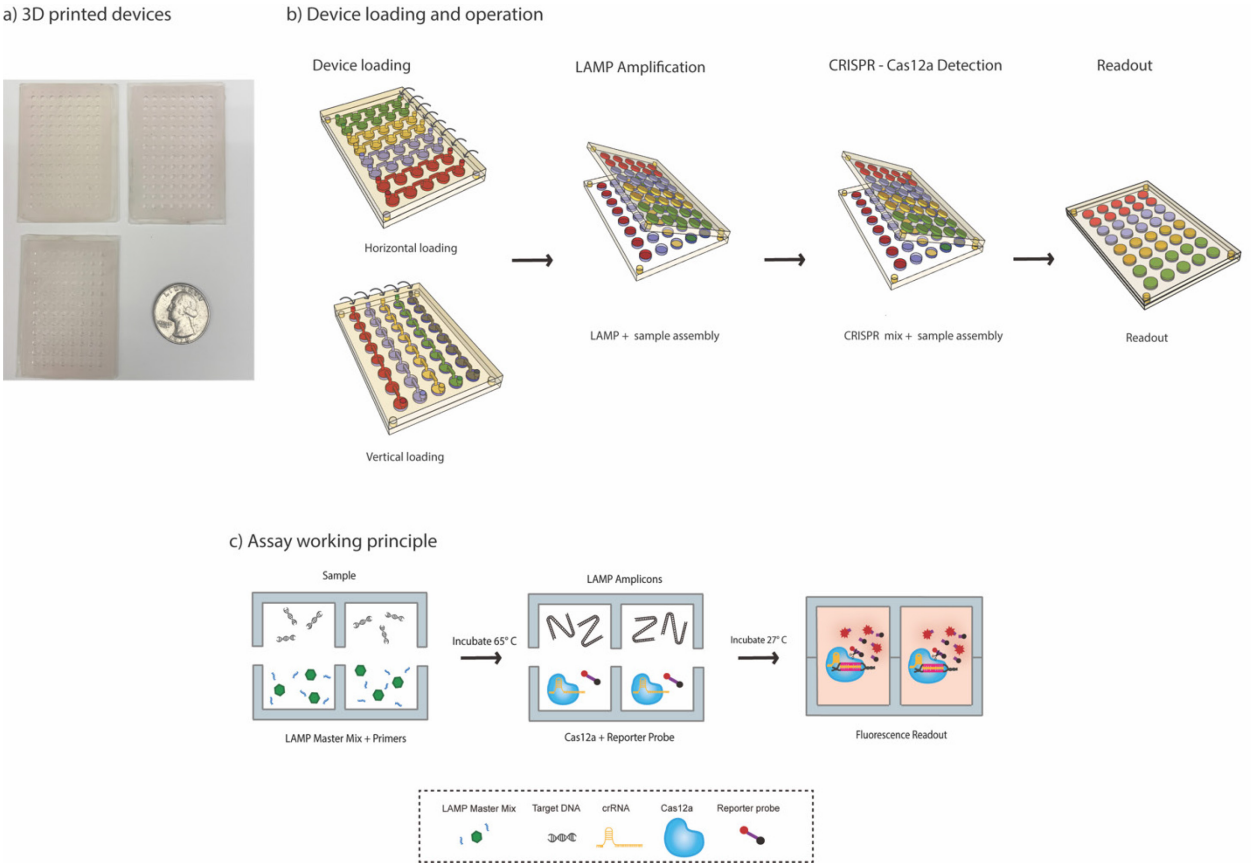

Figure 1. a) An image of 3D printed cPlate devices b) Operation schematic of fluid loading and plate assembly c) Working method of multiplexed LAMP amplification and CRISPR-Cas12a detection in the cPlate device

The steps of performing LAMP-CRISPR-Cas12a biosensing are as follows: 1) sample plate and LAMP plate loading and assembly 2) LAMP amplification 3) CRISPR-Cas12 plate loading 4) CRISPR-Cas12 and LAMP plate assembly 5) fluorescent readout. The entire cPlate-based LAMP-CRISPR-Cas12a workflow is visualized in Figure 1b and Figure 1c. The samples containing target DNA are loaded into the rows of the sample plate using the horizontally loading channel plate. Then, the respective LAMP mixes were loaded onto the LAMP plate using the vertically loading channel plate. The sample plate and LAMP plate are carefully assembled using the corner holes and posts as a guide. The plates were gently secured using adhesive tape and placed in a thermocycler for 30 minutes to 65°C. After isothermal amplification, the sample and LAMP plates are dissembled, and the LAMP plate is stored in a humified environment until assembly with the CRISPR plate. The CRISPR-Cas12a reaction mix for each target was then vertically loaded into the respective columns on the CRISPR plate. Using the corner holes and posts on the plates as a guide, the LAMP plate and CRISPR are gently assembled,

allowing the fluid from each well to mix with its complimentary well. The two plates were secured together using adhesive tape. Fluorescent measurements were acquired every 5 minutes for 30 minutes to read out the result.

Validation of the Loading and Fluid Manipulation

Before applying the cPlate for multiplexed nucleic acid detection, we validated fluid manipulation and reaction feasibility in the device. First, consistent well volume is needed to ensure uniform amplification and signal generation. Both LAMP and CRISPR readout are highly sensitive to reagent availability and concentration. A large deviation in well volume for a single sample would result in high standard deviations in the result. Volume consistency was validated by loading the cPlate with Amplex red and reading the fluorescence profile. As shown in Figure 2a, the fluorescence intensity is uniform across loading paths, with a coefficient of variation (CV) of 4.4%. The loading steps were assessed by loading rows and columns using dye solutions. By visual inspection, we see there is no dye merger between wells or residual fluid in the spaces between wells (Figure 2b). The superhydrophobic coating and microgroove structures on the device sufficiently prevent liquid from remaining between wells and merging with other rows and columns.

Next, the cPlate allows for CRISPR multiplexing by compartmentalizing target reactions into individual wells. Accurate fluid manipulation in the cPlate is critical for effective multiplexing, so reactions do not cross-contaminate and yield false positives. We first validated fluid manipulation by conducting LAMP and CRISPR reactions within the cPlate for a single target and non-template control. For LAMP, a single concentration of cholera genomic DNA was loaded into 3 rows the sample plate and 3 rows were loaded with DI water as a non-template control. The LAMP master mix including the intercalating dye was vertically loaded into the LAMP plate. The plates were assembled and incubated at 65°C for 30 minutes. After incubation the fluorescence intensity for each well was measured. Positive rows containing cholera amplicons yielded fluorescent intensity indicating successful LAMP amplification. The fluorescence intensity for each positive row was averaged and showed no significant difference in intensity (Figure 2d). This indicates that across rows and wells LAMP amplification is uniform. For negative rows, fluorescence intensity was significantly lower than the positive rows, indicating no amplification or liquid merger from positive rows. We then evaluated the CRISPR-Cas12a reaction. Following the above protocol, the LAMP plate containing LAMP mix and sample plate containing cholera samples and non-template controls were assembled and incubated. After amplification, the CRIPSR plate was loaded vertically with respective RNPs and fluorescent probe and assembled. Positive rows resulted in fluorescence intensity while negative rows remained low intensity. Again, the mean fluorescence intensity across rows was not significantly different, showing that fluid manipulation for the entire workflow is accurate (Figure 2e). Because negative rows did not yield high fluorescence intensity for both LAMP and CRISPR-Cas12a reactions, there was no fluid crossover during loading and plate assembly. This is attributed to the superhydrophobic coating and groove structures that confine fluid to their respective wells during loading, assembly, and disassembly. In summary, fluid manipulation within the cPlate is precise and uniform with well intensity CV < 5%, which enables reproducible LAMP and CRISPR reactions across the device.

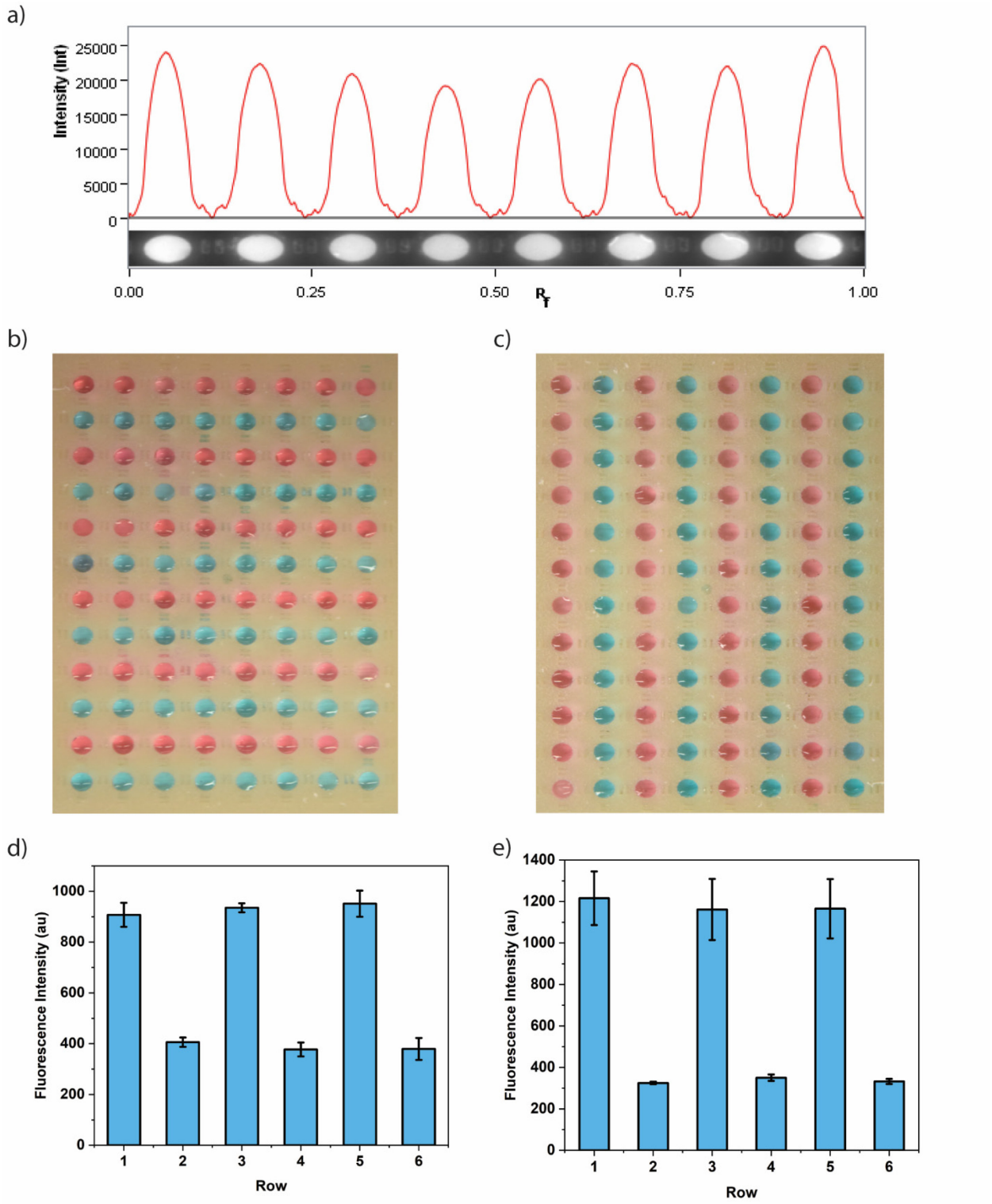

Figure 2. a) Quantitative fluorescence cross section along cPlate. b) image of cPlate row loading. c) image of cPlate column loading row. d) Validation of LAMP reaction in cPlate. Positive control: row 1, 3, and 5; Negative control: row 2, 4, and 6. e) validation of Cas12a reaction in cPlate. Positive control: row 1, 3, and 5; Negative control: row 2, 4, and 6.

LAMP Assay Validation

Prior to coupling LAMP with Cas12a recognition, the LAMP method and primers were validated using SYBR Green intercalating dye detection and gel electrophoresis. LAMP amplicons are confirmed in Figure S3a by gel electrophoresis, where Lane 1 is the ladder and Lanes 3-7 are the waterborne pathogen targets. To complement the gel electrophoresis results, the intercalating dye was added to the LAMP reactions for fluorescence measurement. The fluorescence intensity of the LAMP reaction was measured for each target reaction and non-template control. The non-template control sample contained all target primers to ensure that the primers did not yield false positives. In Figure S3b, LAMP reactions containing target DNA exhibit 90 times higher fluorescent intensity, indicating the presence of LAMP amplicons due to the intercalating dye binding with the growing DNA amplicons during amplification.

Temperature stability of the cPlate device during LAMP amplification

We then demonstrated that liquid evaporation was insignificant during 65°C LAMP reaction. The device was loaded with a fluorescent dye solution and the fluorescence intensity was measured across the wells. The device was then heated to 65°C for 30 minutes and the fluorescence intensity was measured. As shown in Figure S4 there is an insignificant change in the average fluorescent intensity, indicating minimal liquid evaporation from the device. In addition to low fluid evaporation, the device polymer material and superhydrophobic coating were stable at 65°C.

Evaluation of the CRISPR-Cas12a Assay for cross-reactivity

To ensure crRNA specificity and demonstrate device feasibility for multiplexing, we conducted a cross-reactivity assay by analyzing the four targets simultaneously in the cPlate. This assay evaluated whether non-specific Cas12a activity occurs in non-target sample wells. Each column of the CRISPR well plate was loaded with a single target CRISPR reaction mix and the sample well plate rows were each loaded with a single target LAMP amplicon. A row loaded with a four-target mixture was included as a positive control and a row was loaded with NEBuffer™ r2.1to serve as the non-template control. The loading pattern can be visualized in Figure S2. The two plates were assembled and after 30 minutes of room temperature incubation, the fluorescence intensities for all wells were collected. The wells that contained complimentary CRISPR-Cas12a reaction mix, and LAMP amplicon target generated high signal intensity, while the mix-matched wells generated signals comparable to the blank. (Figure 3a) These results confirm the high specificity of the CRISPR-Cas12 assay and that target DNA regions do not interfere.

Investigation of the Waterborne Pathogen CRISPR-Cas12a Assay Reaction Conditions

To ensure maximum performance of the LAMP + CRISPR-Cas12a reaction, the reaction was first optimized by adjusting key reaction conditions including the concentrations of fluorescence reporter and RNP, respectively. Systematically optimizing reaction parameters, such as temperature, buffer composition, reporter concentration, and RNP concentration, have improved assay sensitivity and reaction rate.[25,26] Because CRISPR-Cas reactions follow Michaelis-Menten kinetics, the LOD is primarily governed by k_{cat} and

K_m.[25,27,28] Both are influenced by the amount of substrate availability. CRISPR-Cas12a reactions are measured using either endpoint or velocity measurement to distinguish between positive and negative samples. In this work, we chose to endpoint-based measurement where a measurement statistically different from the blank by 3 standard deviations is considered a positive result. This detection scheme enables shorter detection time with maintained sensitivity.

First, the concentration L.b. Cas12:crRNA, or the ribonucleoprotein (RNP), was optimized. As demonstrated in other works[3,12,17], the concentration of crRNA exceeds that of Cas12 to ensure adequate Cas12a and crRNA binding; therefore, a ratio of 1:1.25 was used across all reactions. Two different RNP concentrations were evaluated by using a constant target DNA concentration, fluorescent probe concentration, and LAMP conditions. As shown in Figure 3b, increasing the concentration of RNP from 275 nM to 680 nM resulted in 5 times greater fluorescence intensity after 30 minutes of incubation. While increasing the concentration of RNP from 680 nM to 1 μM yield improved fluorescence intensity two-fold, this higher concentration of RNP resulted in rapid consumption of the Cas12a reagent. In our work, the balance of overall cost and performance was carefully considered. The RNP concentration at 680 nM was selected to maintain good assay performance while reducing overall assay cost. Additionally, the 680 nM RNP is concentration consistent with other established CRISPR assays.[29–31]

We then optimized the concentration of fluorescent reporter probe by varying its concentration from 1 μM to 6 μM in the CRISPR-Cas12a reaction mix (Figure 3c). Typically, in CRISPR-Cas12a reactions, the fluorescence intensity will plateau over time due the consumption of the fluorescence reporter. The increased concentration of the fluorescent reporter increased the signal generated from the reaction because of the higher reporter availability. Five concentrations of fluorescent probe were evaluated using a constant target DNA concentration, RNP concentration, and LAMP conditions. 1.25 μM to 2 μM fluorescence probe yielded similar results, while 4.75 μM probe yielded in 4 times greater intensity. When the concentration of probe was further increased to 6 μM, the resulting intensity was not significantly different from 4.75 μM, so 4.75 μM was selected as the optimized probe condition.

By using the optimized conditions of 680 nM RNP and 4.75 μM fluorescent probe the fluorescence signal generation for 1 ng/mL of DNA target was improved to the same magnitude as 100 ng/mL target (Figure 3d) with 275 nM RNP and 2 μM fluorescent probe. This demonstrates that optimization improves fluorescent output and detection sensitivity.

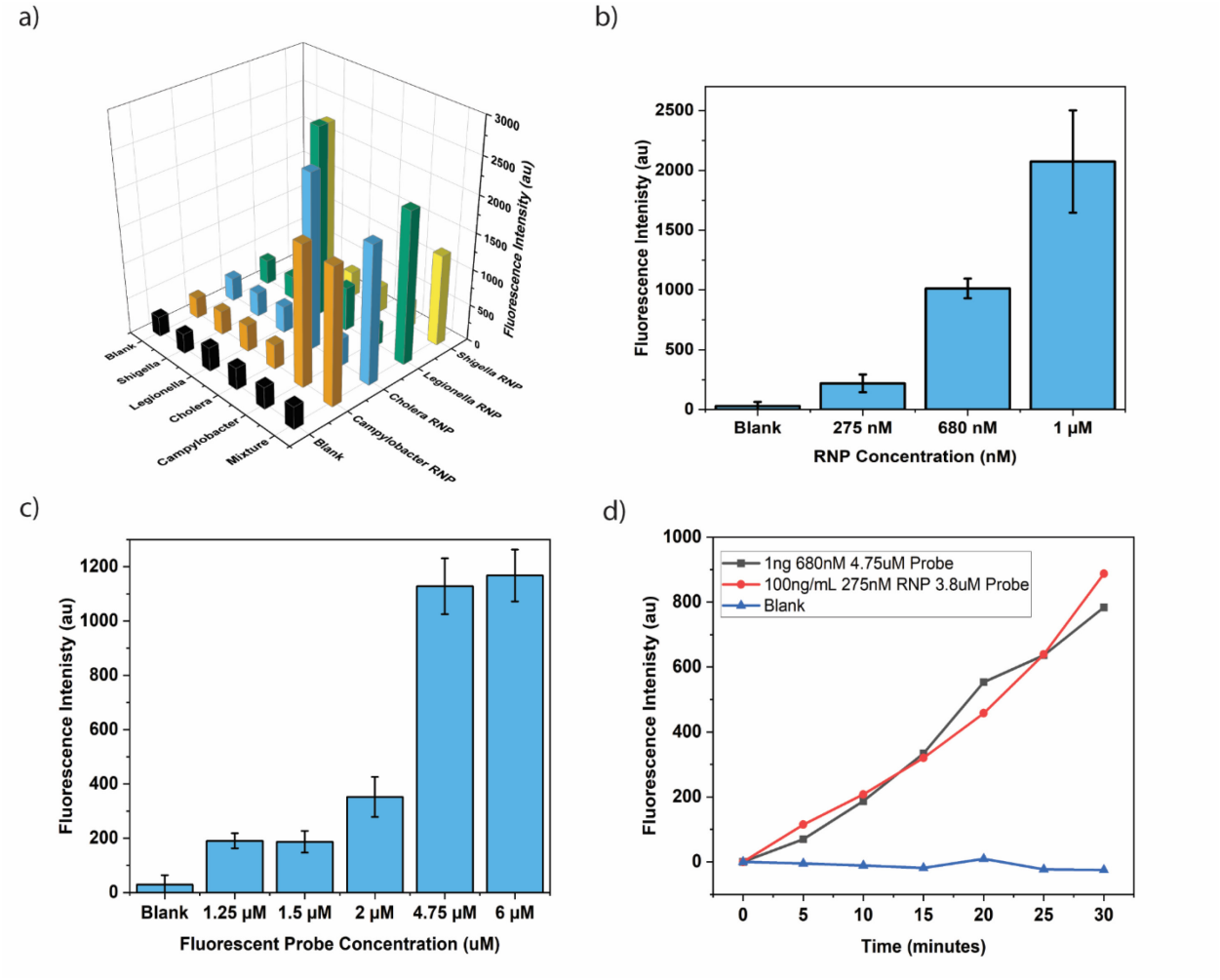

Figure 3. Optimization of the multiplexed assay. a) evaluation of crRNA cross-reactivity of 4 targets. X axis: DNA sample, Z axis: RNP complex, Y axis: fluorescence intensity b) Fluorescence intensity at different RNP concentrations (0 nM, 275 nM, and 680 nM, and 1 µM). c) Fluorescence intensity at different fluorescent reporter probe concentrations (0 µM, 1.25 µM, 1.5 µM, 2 µM, and 4.75 µM). d) Real-time fluorescence measurement of the optimized assay for 1 ng/mL of target vs. unoptimized assay for 100 ng/mL of target. Values represent the mean ± SD of three independent experiments.

Evaluation of the Optimized CRISPR-Cas12a Assay in the cPlate for a multiplexed detection

To demonstrate the multiplexing ability of the device, campylobacter, cholera, shigella, and legionella were selected as these are often screened together as common waterborne pathogen targets. These bacteria are among those that cause serious gastrointestinal infections associated with consuming contaminated drinking water. Target genes for each pathogen are shown in Table S1 and are conserved genes across strains. The four nucleic acids were detected simultaneously on a single cPlate device. Each target was assessed for 1 fg/mL to 1 ng/mL of target genomic DNA to generate the

response curves shown in Figure 4 a-d, while Figures S6 and S7 show the real-time fluorescence curves for representative samples

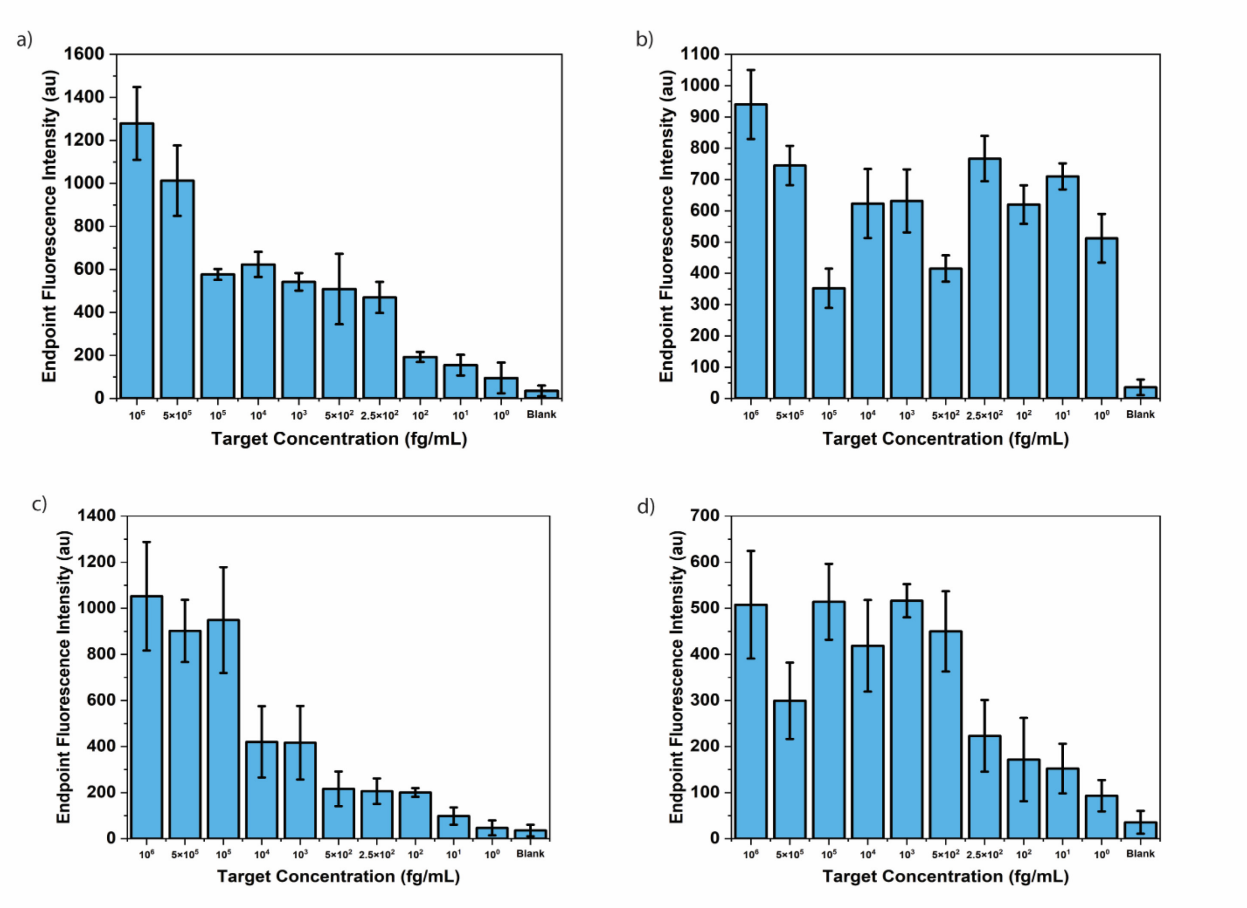

Figure 4. Performance evaluation of the optimized multiplexed assay for a) shigella b) legionella c) cholera d) campylobacter. Values represent the mean ± SD of three independent experiments.

To determine analytical sensitivity, we utilized endpoint fluorescence measurement. The endpoint was quantified as the time required to achieve a threshold that is greater than three times the signal-to-noise of the non-template control. For all targets, 30 minutes was selected as the endpoint needed to quantify a positive result compared to the control (Figure S5). The 30-minute incubation time is selected to keep an entire assay time at ~1 hour while providing high-sensitivity measurement.

The fluorescence intensity yielded in CRISPR reactions is governed by the target concentration available to trigger *trans*-cleavage. It is expected that decreasing the sample concentration will eventually result in a decrease in the fluorescence signal. As the decreasing concentration yields lower intensities, we can estimate the sensitivity as the lowest concentration that is significantly higher than the blank. The fluorescence intensities are not linearly correlated and show some variation, especially at higher DNA concentrations. This is attributed to variations in the fluorescence intensity when using

freshly prepared reagents and conducting assays across multiple days and devices. As shown in Figure S7, fluorescence intensity decreases when stock solutions are reused with more than 24 hours between experiments.

Compared to other reported CRISPR-Cas12a biosensing technology[9,17,32–35] for single DNA targets, our device demonstrates comparable high sensitivity measurements to the fg/mL level of starting genetic material, while allowing simultaneous detection of multiple targets with physical separation. The limits of detection for each target were found to be 10 fg/mL shigella, 1 fg/mL legionella, 10 fg/mL cholera, and 1 fg/mL campylobacter. Assay sensitivity can be further improved by optimizing LAMP primer and crRNA sequences since the sequences determine the amplification yield and crRNA and target region binding efficacy. For example, we optimized the crRNA sequence for the Legionella assay, which improved the LOD (Figure S8). In this work, 48 reactions were performed using a single cPlate device, which consists of 2 replicates of the 4 individual targets, one 4-plex mixture, and one negative control. Because of the working principle of cPlate-based fluid manipulation, the present device is very scalable. More reactions and targets can be easily added to further expand the screening panel or for handling multiple samples.

Conclusion

We present the cPlate-based method for CRISPR-Cas12a detection of four waterborne pathogens. Because of the microfluidic loading system and physical separation of targets, this device enables simple multiplexing. The device achieved low fg/mL level of LODs for all four targets. In addition, the entire reaction is completed within one hour without the need for external fluid manipulation equipment. The device is simple to operate, reduces the number of manual steps required for multiplexing, and measures multiple samples in replicate. We successfully demonstrated the feasibility of the cPlate device for screening a panel of pathogens.

The CRISPR-Cas12a recognition offers a high level of versatility for biosensing applications. crRNA offers a “plug and play” design, where the target DNA sequence can be easily modified by changing the crRNA sequence. This advantage, coupled with the cPlate well design, offers a multitude of possible designs for future studies. Lastly, because the cPlate is 3D-printed, the devices are simple and cost-effective to fabricate and do not require external pumps or valves for operation. The device design can be easily scaled to increase the number of wells on a single device, thus allowing the number of targets and samples to be modified. Because of the demonstrated sensitivity, specificity, and ease of operation, this device offers desirable performance and easy operation for POC nucleic acid biosensing. These attributes, coupled with flexible crRNA design in CRISPR-Cas12a assays, the multiplexed cPlate device can be further applied to a wide range of genetic targets.

Acknowledgments

This work was partly supported by the National Institute of Health (R01GM135432) and National Science Foundation (ECCS-2144216). KC acknowledges NSF Graduate

Research Fellowship Program (GRFP) grant (#13300542). We acknowledge the use of WVU BioNano Shared Research Facilities.

References

(1) Scheler, O.; Glynn, B.; Kurg, A. Nucleic Acid Detection Technologies and Marker Molecules in Bacterial Diagnostics. *Expert Review of Molecular Diagnostics* **2014**, *14* (4), 489–500.
(2) van Dongen, J. E.; Berendsen, J. T. W.; Steenbergen, R. D. M.; Wolthuis, R. M. F.; Eijkel, J. C. T.; Segerink, L. I. Point-of-Care CRISPR/Cas Nucleic Acid Detection: Recent Advances, Challenges and Opportunities. *Biosensors and Bioelectronics* **2020**, *166*, 112445.
(3) Chen, J. S.; Ma, E.; Harrington, L. B.; Da Costa, M.; Tian, X.; Palefsky, J. M.; Doudna, J. A. CRISPR-Cas12a Target Binding Unleashes Indiscriminate Single-Stranded DNase Activity. *Science* **2018**, *360* (6387), 436–439.
(4) Gootenberg, J. S.; Abudayyeh, O. O.; Lee, J. W.; Essletzbichler, P.; Dy, A. J.; Joung, J.; Verdine, V.; Donghia, N.; Daringer, N. M.; Freije, C. A.; Myhrvold, C.; Bhattacharyya, R. P.; Livny, J.; Regev, A.; Koonin, E. V.; Hung, D. T.; Sabeti, P. C.; Collins, J. J.; Zhang, F. Nucleic Acid Detection with CRISPR-Cas13a/C2c2. *Science* **2017**, *356* (6336), 438–442.
(5) Kaminski, M. M.; Abudayyeh, O. O.; Gootenberg, J. S.; Zhang, F.; Collins, J. J. CRISPR-Based Diagnostics. *Nat Biomed Eng* **2021**, *5* (7), 643–656.
(6) Zavvar, T. S.; Khoshbin, Z.; Ramezani, M.; Alibolandi, M.; Abnous, K.; Taghdisi, S. M. CRISPR/Cas-Engineered Technology: Innovative Approach for Biosensor Development. *Biosensors and Bioelectronics* **2022**, *214*, 114501.
(7) Xu, Z.; Chen, D.; Li, T.; Yan, J.; Zhu, J.; He, T.; Hu, R.; Li, Y.; Yang, Y.; Liu, M. Microfluidic Space Coding for Multiplexed Nucleic Acid Detection via CRISPR-Cas12a and Recombinase Polymerase Amplification. *Nat Commun* **2022**, *13* (1), 6480.
(8) Kanitchinda, S.; Srisala, J.; Suebsing, R.; Prachumwat, A.; Chaijarasphong, T. CRISPR-Cas Fluorescent Cleavage Assay Coupled with Recombinase Polymerase Amplification for Sensitive and Specific Detection of Enterocytozoon Hepatopenaei. *Biotechnology Reports* **2020**, *27*, e00485.
(9) Tsou, J.-H.; Leng, Q.; Jiang, F. A CRISPR Test for Detection of Circulating Nuclei Acids. *Translational Oncology* **2019**, *12* (12), 1566–1573.
(10) Mukama, O.; Wu, J.; Li, Z.; Liang, Q.; Yi, Z.; Lu, X.; Liu, Y.; Liu, Y.; Hussain, M.; Makafe, G. G.; Liu, J.; Xu, N.; Zeng, L. An Ultrasensitive and Specific Point-of-Care CRISPR/Cas12 Based Lateral Flow Biosensor for the Rapid Detection of Nucleic Acids. *Biosensors and Bioelectronics* **2020**, *159*, 112143.
(11) Pang, B.; Xu, J.; Liu, Y.; Peng, H.; Feng, W.; Cao, Y.; Wu, J.; Xiao, H.; Pabbaraju, K.; Tipples, G.; Joyce, M. A.; Saffran, H. A.; Tyrrell, D. L.; Zhang, H.; Le, X. C. Isothermal Amplification and Ambient Visualization in a Single Tube for the Detection of SARS-CoV-2 Using Loop-Mediated Amplification and CRISPR Technology. *Anal. Chem.* **2020**, *92* (24), 16204–16212.
(12) Wang, R.; Qian, C.; Pang, Y.; Li, M.; Yang, Y.; Ma, H.; Zhao, M.; Qian, F.; Yu, H.; Liu, Z.; Ni, T.; Zheng, Y.; Wang, Y. OpvCRISPR: One-Pot Visual RT-LAMP-CRISPR

Platform for SARS-Cov-2 Detection. *Biosensors and Bioelectronics* **2021**, *172*, 112766.
(13) Blanluet, C.; Huyke, D. A.; Ramachandran, A.; Avaro, A. S.; Santiago, J. G. Detection and Discrimination of Single Nucleotide Polymorphisms by Quantification of CRISPR-Cas Catalytic Efficiency. *Anal. Chem.* **2022**, *94* (43), 15117–15123.
(14) Choi, J.-H.; Lim, J.; Shin, M.; Paek, S.-H.; Choi, J.-W. CRISPR-Cas12a-Based Nucleic Acid Amplification-Free DNA Biosensor via Au Nanoparticle-Assisted Metal-Enhanced Fluorescence and Colorimetric Analysis. *Nano Lett.* **2021**, *21* (1), 693–699.
(15) Li, F.; Ye, Q.; Chen, M.; Zhou, B.; Zhang, J.; Pang, R.; Xue, L.; Wang, J.; Zeng, H.; Wu, S.; Zhang, Y.; Ding, Y.; Wu, Q. An Ultrasensitive CRISPR/Cas12a Based Electrochemical Biosensor for Listeria Monocytogenes Detection. *Biosensors and Bioelectronics* **2021**, *179*, 113073.
(16) Mahas, A.; Hassan, N.; Aman, R.; Marsic, T.; Wang, Q.; Ali, Z.; Mahfouz, M. M. LAMP-Coupled CRISPR–Cas12a Module for Rapid and Sensitive Detection of Plant DNA Viruses. *Viruses* **2021**, *13* (3), 466.
(17) Wang, B.; Wang, R.; Wang, D.; Wu, J.; Li, J.; Wang, J.; Liu, H.; Wang, Y. Cas12aVDet: A CRISPR/Cas12a-Based Platform for Rapid and Visual Nucleic Acid Detection. *Anal. Chem.* **2019**, *91* (19), 12156–12161.
(18) Broughton, J. P.; Deng, X.; Yu, G.; Fasching, C. L.; Servellita, V.; Singh, J.; Miao, X.; Streithorst, J. A.; Granados, A.; Sotomayor-Gonzalez, A.; Zorn, K.; Gopez, A.; Hsu, E.; Gu, W.; Miller, S.; Pan, C.-Y.; Guevara, H.; Wadford, D. A.; Chen, J. S.; Chiu, C. Y. CRISPR–Cas12-Based Detection of SARS-CoV-2. *Nat Biotechnol* **2020**, *38* (7), 870–874.
(19) Gootenberg, J. S.; Abudayyeh, O. O.; Kellner, M. J.; Joung, J.; Collins, J. J.; Zhang, F. Multiplexed and Portable Nucleic Acid Detection Platform with Cas13, Cas12a, and Csm6. *Science* **2018**, *360* (6387), 439–444.
(20) Bruch, R.; Urban, G. A.; Dincer, C. CRISPR/Cas Powered Multiplexed Biosensing. *Trends in Biotechnology* **2019**, *37* (8), 791–792.
(21) Li, Y.; Liu, L.; Liu, G. CRISPR/Cas Multiplexed Biosensing: A Challenge or an Insurmountable Obstacle? *Trends in Biotechnology* **2019**, *37* (8), 792–795.
(22) Ackerman, C. M.; Myhrvold, C.; Thakku, S. G.; Freije, C. A.; Metsky, H. C.; Yang, D. K.; Ye, S. H.; Boehm, C. K.; Kosoko-Thoroddsen, T.-S. F.; Kehe, J.; Nguyen, T. G.; Carter, A.; Kulesa, A.; Barnes, J. R.; Dugan, V. G.; Hung, D. T.; Blainey, P. C.; Sabeti, P. C. Massively Multiplexed Nucleic Acid Detection with Cas13. *Nature* **2020**, *582* (7811), 277–282.
(23) Hu, T.; Ke, X.; Li, W.; Lin, Y.; Liang, A.; Ou, Y.; Chen, C. CRISPR/Cas12a-Enabled Multiplex Biosensing Strategy Via an Affordable and Visual Nylon Membrane Readout. *Advanced Science* **2023**, *10* (2), 2204689.
(24) He, Z.; Huffman, J.; Curtin, K.; Garner, K. L.; Bowdridge, E. C.; Li, X.; Nurkiewicz, T. R.; Li, P. Composable Microfluidic Plates (CPlate): A Simple and Scalable Fluid Manipulation System for Multiplexed Enzyme-Linked Immunosorbent Assay (ELISA). *Anal. Chem.* **2021**, *93* (3), 1489–1497.
(25) Hsieh, K.; Zhao, G.; Wang, T.-H. Applying Biosensor Development Concepts to Improve Preamplification-Free CRISPR/Cas12a-Dx. *Analyst* **2020**, *145* (14), 4880–4888.

(26) Yue, H.; Shu, B.; Tian, T.; Xiong, E.; Huang, M.; Zhu, D.; Sun, J.; Liu, Q.; Wang, S.; Li, Y.; Zhou, X. Droplet Cas12a Assay Enables DNA Quantification from Unamplified Samples at the Single-Molecule Level. *NANO LETTERS* **2021**, *21* (11), 4643–4653.
(27) Nalefski, E. A.; Patel, N.; Leung, P. J. Y.; Islam, Z.; Kooistra, R. M.; Parikh, I.; Marion, E.; Knott, G. J.; Doudna, J. A.; Le Ny, A.-L. M.; Madan, D. Kinetic Analysis of Cas12a and Cas13a RNA-Guided Nucleases for Development of Improved CRISPR-Based Diagnostics. *iScience* **2021**, *24* (9), 102996.
(28) Ramachandran, A.; Santiago, J. G. CRISPR Enzyme Kinetics for Molecular Diagnostics. *Anal. Chem.* **2021**, *93* (20), 7456–7464.
(29) Bai, L.; Wang, L.; Huang, S.; Bai, R.; Lv, X.; Sun, L.; Zhang, F.; Xu, X. Rapid, Visual, and Sequence-Specific Detection of *Salmonella* in Egg Liquid with Vis-NEAA, a CRISPR/Cas12 Empowered New Strategy. *J. Agric. Food Chem.* **2022**, *70* (7), 2401–2409.
(30) Li, Z.; Ding, X.; Yin, K.; Avery, L.; Ballesteros, E.; Liu, C. Instrument-Free, CRISPR-Based Diagnostics of SARS-CoV-2 Using Self-Contained Microfluidic System. *Biosensors and Bioelectronics* **2022**, *199*, 113865.
(31) Ali, Z.; Aman, R.; Mahas, A.; Rao, G. S.; Tehseen, M.; Marsic, T.; Salunke, R.; Subudhi, A. K.; Hala, S. M.; Hamdan, S. M.; Pain, A.; Alofi, F. S.; Alsomali, A.; Hashem, A. M.; Khogeer, A.; Almontashiri, N. A. M.; Abedalthagafi, M.; Hassan, N.; Mahfouz, M. M. ISCAN: An RT-LAMP-Coupled CRISPR-Cas12 Module for Rapid, Sensitive Detection of SARS-CoV-2. *Virus Research* **2020**, *288*, 198129.
(32) He, Q.; Yu, D.; Bao, M.; Korensky, G.; Chen, J.; Shin, M.; Kim, J.; Park, M.; Qin, P.; Du, K. High-Throughput and All-Solution Phase African Swine Fever Virus (ASFV) Detection Using CRISPR-Cas12a and Fluorescence Based Point-of-Care System. *Biosensors and Bioelectronics* **2020**, *154*, 112068.
(33) Chen, Z.; Li, J.; Li, T.; Fan, T.; Meng, C.; Li, C.; Kang, J.; Chai, L.; Hao, Y.; Tang, Y.; Al-Hartomy, O. A.; Wageh, S.; Al-Sehemi, A. G.; Luo, Z.; Yu, J.; Shao, Y.; Li, D.; Feng, S.; Liu, W. J.; He, Y.; Ma, X.; Xie, Z.; Zhang, H. A CRISPR/Cas12a-Empowered Surface Plasmon Resonance Platform for Rapid and Specific Diagnosis of the Omicron Variant of SARS-CoV-2. *National Science Review* **2022**, *9* (8), nwac104.
(34) Yu, T.; Zhang, S.; Matei, R.; Marx, W.; Beisel, C. L.; Wei, Q. Coupling Smartphone and CRISPR–Cas12a for Digital and Multiplexed NUCLEIC ACID Detection. *AIChE J* **2021**, *67* (12).
(35) Sullivan, T. J.; Dhar, A. K.; Cruz-Flores, R.; Bodnar, A. G. Rapid, CRISPR-Based, Field-Deployable Detection Of White Spot Syndrome Virus In Shrimp. *Sci Rep* **2019**, *9* (1), 19702.